PREDICTION OF PORCELAIN TILE FINAL DIMENSIONS FROM NON-DESTRUCTIVE BULK DENSITY MEASUREMENT

J. Boix; J. Balaguer; J. M. Tiscar; A. Olmedilla

Instituto de Tecnología Cerámica (ITC). Asociación de Investigación de las Industrias Cerámicas (AICE).
Universitat Jaume I. Castellón. Spain.

ABSTRACT

Porcelain tile shrinkage during firing is very high and, in addition, exhibits great variability with the dry bulk density defined in the forming stage. Such behaviour of the material requires thorough control of the manufacturing process to assure good dimensional stability of the finished product.

Non-destructive measurement of bulk density by X-ray absorption has proven to be a suitable technique for controlling the ceramic tile forming process. This study examines the use of thickness and bulk density distribution maps obtained by this technique of industrial tile bodies, for feeding software for predicting viscous sintering based on the finite element technique and the SOVS (Skorohod–Olevsky viscous sintering) constitutive model. The finite element simulation software thus becomes an extremely useful tool for porcelain tile manufacture, as it allows the material's behaviour during firing to be anticipated.

The proposed methodology has been validated on an industrial level, evidencing its potential for improving industrial manufacturing process control for this type of product.

1. INTRODUCTION

In recent years porcelain tile has become one of the most highly sought-after ceramic products because of its excellent technical performance and aesthetic qualities, many of which are related to the high densification resulting from liquid-phase sintering during tile firing[1]. In this physical process, tile reduction in porosity is often accompanied by shrinkage of over 7% which, as reported in different [2], mainly depends on dry bulk density, defined in forming, and on peak firing temperature. To assure good dimensional stability of the finished product, careful control of the forming operation is essential. Indeed, control during the pressing stage of critical variables such as spray-dried powder moisture content and tile body bulk density is key to obtaining a product with the desired physical [3].The relationships between a material's forming conditions and firing behaviour have long been known, so that tile behaviour during firing may be induced. However, in a great number of companies, control of the forming process is complemented by firing trials of unglazed bodies. These complementary controls seek, fundamentally, to detect problems relating to departures from rectangularity in the tile and/or differences in calibre between tiles obtained in the same pressing cycle. Performing such complementary controls is a complex task, as the production flow needs to be interrupted and a kiln needs to be available with the appropriate firing cycle. An alternative to firing controls would be prediction of the behaviour that tile bodies would have from their green properties, for given processing conditions.

A previous study [4] examined the possibility of reproducing porcelain tile densification during tile firing by means of the Skorohod-Olevsky viscous sintering (SOVS) model defined by equations (1) and (2).

$$\dot{\epsilon}_{ij}^{in} = \frac{\sigma'_{ij}}{2\eta_0\phi} + \frac{\sigma_{kk} - 3\sigma_s}{18\eta_0\varphi\psi}\delta_{ij} \qquad (1)$$

$$\frac{\dot{\rho}_r}{\rho_r} = -\dot{\epsilon}_{kk}^{in} \qquad (2)$$

where, $\dot{\epsilon}_{ij}^{in}$ is the inelastic strain rate tensor, σ'_{ij} the deviatoric component of the stress tensor, σ_{kk} the trace of the stress tensor, σ_s the effective sintering stress, ϕ and ψ normalised shear viscosity and normalised volumetric viscosity of the material, which depend on relative density (ρ_r), η_0 apparent viscosity and δ_{ij} the Kronecker delta. Finally, $\dot{\rho}_r$ is the rate of variation of ρ_r, while $\dot{\epsilon}_{kk}^{in}$ is the trace of the inelastic strain rate tensor.

It may be noted that the original SOVS model did not explicitly include the effect of grain growth during sintering, which is why Argüello et al. [5] included it in phenomenological form in apparent viscosity itself.

Thus, the grain growth proposed by Argüello et al. has been directly incorporated into equation (1) through parameter φ, which depends on ρ_r and represents the volumetric relationship between grain size at a given instant and the initial grain size of the composition.

The solution of this constitutive model involves previously knowing the evolution with temperature of the thermal properties of the material and having a viscous law that appropriately describes how its viscosity varies during firing. The thermal characterisation of the material has been addressed elsewhere [4] [[8]. However, for the viscous law, an equation of the Arrhenius type is generally resorted to. Unfortunately, it has been verified that this law does not allow proper reproduction of the complex physical phenomena that develop during liquid-phase sintering in porcelain tile bodies [4]. A reasonable alternative would involve assuming an additive viscous law that envisages crystalline phase change mechanisms, mullite crystallisation and quartz dissolution [1], which occur in the liquid phase in the range between 950 and 1100ºC. However, no theory has been developed to date that envisages an additive viscous law with these sintering mechanisms. For this reason, in this study an experimental viscous law, obtained from a multiparameter fit of equation (1), has been used.

Knowing the thermo-mechanical parameters described above, starting with the geometry of a green ceramic tile and its bulk density distribution, and using a numerical method such as that of finite elements, tile geometry and bulk density distribution, after the tile has undergone a given thermal cycle, can be obtained. In this study, it is therefore sought to validate the methodology outlined in Figure 1, which would allow product behaviour during firing to be anticipated, minimising or supressing the complementary firing controls customarily carried out by the companies.

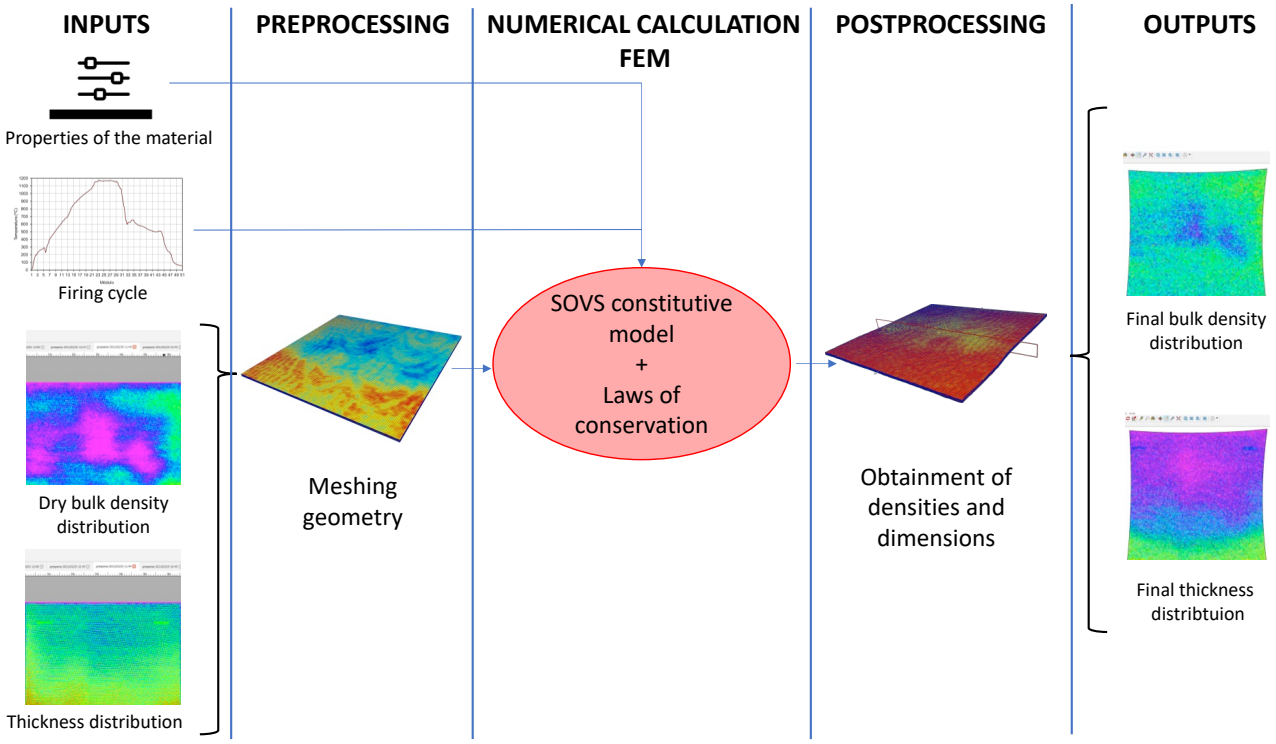

***Figure 1**.Scheme of the methodology proposed for reproducing porcelain tile behaviour during firing (deformations magnified for illustrative purposes).*

The proposed methodology starts with bulk density and thickness distribution maps of porcelain tile obtained by non-destructive inspection using X-ray absorption [6]. These data, together with the external dimensions of the tile and its thermo-mechanical properties, determined in a preliminary laboratory characterisation, are entered into a numerical simulation program by finite elements through the Salome–Meca software, which solves the SOVS model and the conservation equations for the thermal cycle with which the tile is processed. The calculation yields tile bulk density distribution and geometry, including both the expected thickness and dimensions of the sides of the tile after firing.

2. EXPERIMENTAL PROCEDURE

To validate the proposed method, on the one hand, it was sought to reproduce the behaviour of a porcelain tile composition subjected to a series of dilatometric tests, which in turn allows a viscous law to be obtained. On the other hand, the proposed control procedure was verified on porcelain tiles processed under industrial conditions, made from the same composition. The materials used and the experimental procedure followed in these experiments are described below.

2.1. MATERIALS

The study was carried out with a spray-dried powder composition customarily used in porcelain tile manufacture. With a view to establishing its optimum processing conditions, its compaction diagram and its vitrification diagram were determined. According to these diagrams, the optimum firing range of the composition was 1190±5ºC, at a forming dry bulk density of 1950 ± 5 kg/m^3.

In addition, following the procedure described in [4], its thermal conductivity was obtained, which was 0.6 W/(m K), for an assumed constant calorific capacity equal to 1250 J/(kg K).

2.2 OBTAINMENT OF THE VISCOUS LAW

With a view to obtaining a viscous law that allowed the material's behaviour to be reproduced during sintering, dilatometric analysis of the composition for different degrees of starting compaction (ρ_0) was carried out. Green test pieces measuring 30 mm x 5 mm x 5 mm were formed at three different dry bulk densities and their densification was recorded using a contact dilatometer.

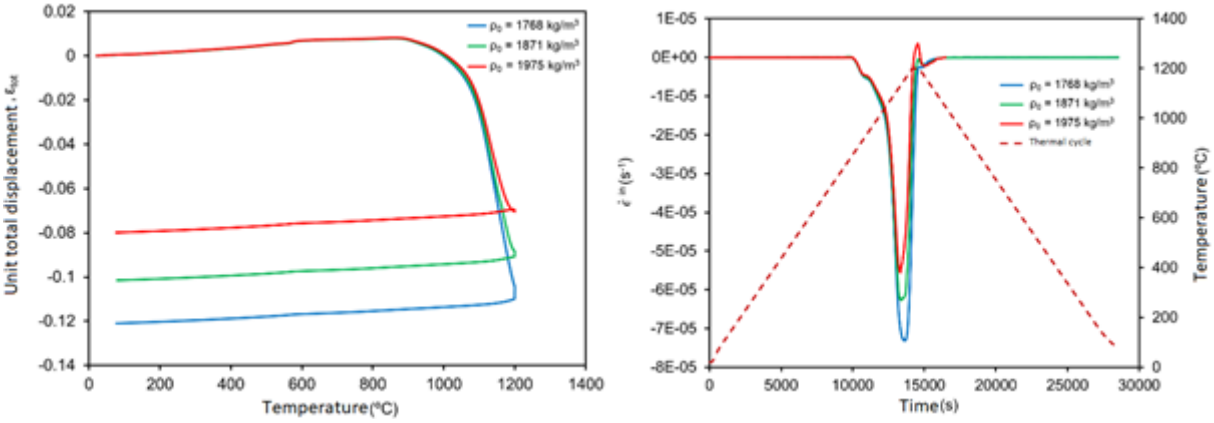

Figure 2. *Left: dilatometric plots of three porcelain tile test pieces at three different initial densities. Right: rate of inelastic strain and thermal cycle of three test pieces with different initial bulk density, obtained from the dilatometric plots.*

The three dilatometric plots are shown in Figure 2 (left). These allow calculation of the rate of change of the inelastic component in the direction measured by the dilatometer ($\dot{\epsilon}^{in}$), plotted in Figure 2 (right), together with the thermal cycle used in the tests. Note the overshoot undergone by $\dot{\epsilon}^{in}$ at peak temperature, which increased with test piece initial density. This phenomenon could be due to the release at high temperature of certain volatile components that generate a minor expansion of the body, slightly altering the usual evolution of shrinkage during the sintering process. In any event, this phenomenon must be omitted to obtain a consistent viscous law.

From the results of these tests, using multiparameter fitting methods, η_0 was obtained from equations (1) and (2), for the relationship proposed by Argüello that relates φ to ρ_r [5]. These tests were subsequently simulated following the methodology proposed in Figure 1 to evidence the correlation between the experimental data and the simulated results considering the proposed viscous law.

2.3 REPRODUCTION OF PORCELAIN TILE BEHAVIOUR UNDER INDUSTRIAL CONDITIONS

To evidence the usefulness of the proposed methodology for controlling the porcelain tile manufacturing process, the behaviour during processing of 4 industrial bodies was simulated. The results of the simulations were compared with the experimental data obtained on processing the bodies. Specifically, the pieces used, with nominal fired dimensions of 600 mm x 600 mm, were moulded by uniaxial pressing in a semi-dry state in an industrial press equipped with a die comprising two cavities. On the one hand, under standard press regulation conditions, the pieces referenced 1 and 2 were obtained in the same pressing cycle, each piece corresponding, respectively, to the die cavity in which it was formed. On the other hand, under the press feed system regulation conditions in which it was sought, voluntarily, to deposit a heterogeneous charge of powder in the cavities, bodies referenced 1X and 2X were prepared.

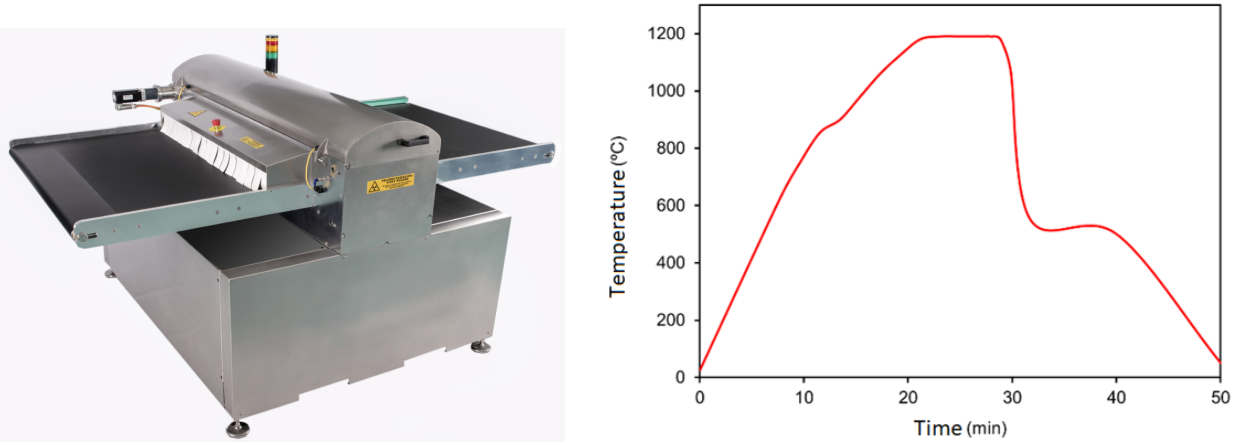

***Figure 3**. Non-destructive bulk density measuring equipment used in the study (left) and industrial thermal cycle used in firing the bodies (right).*

After oven drying at 110ºC to constant weight, the bodies were analysed with a non-destructive bulk density measurement unit using X-ray absorption (Figure 3). After the analysis, their dry bulk density and thickness distribution maps were obtained (Figure 4 and Figure 5). This information, together with the thermo-mechanical properties of the composition and the firing thermal cycle, was used as input variables of the model.

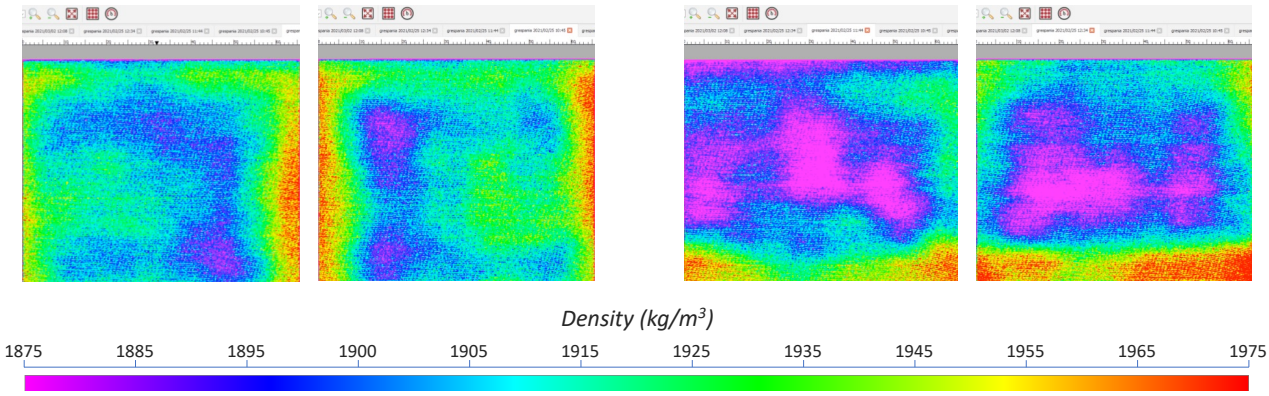

***Figure 4**. Dry bulk density distribution maps of the industrial bodies used in verifying the methodology.*

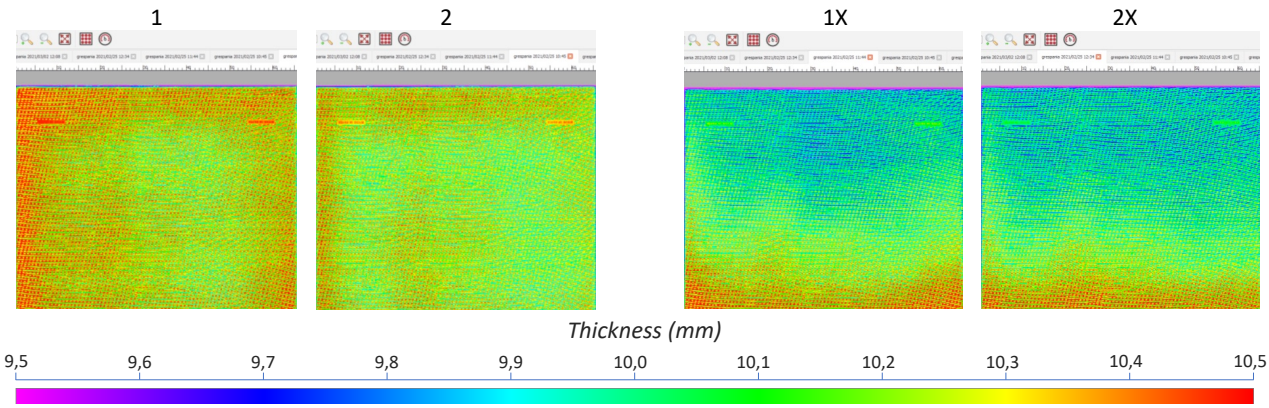

***Figure 5.** Thickness distribution maps of the green industrial bodies used in verifying the methodology.*

As may be observed, the density distribution maps of bodies 1 and 2 were much more uniform than those referenced 1X and 2X. Indeed, the pressing cycle in which the latter pair were formed exhibited a displaced powder feed towards the front part of the cavities (bottom part of the maps) in order to simulate a possible charge defect during the forming process. This heterogeneity in the charge was also transferred to the green thickness maps, in which both body 1X and 2X exhibited a greater thickness in their front part.

Finally, the dry bodies were fired in an industrial roller kiln fitted with natural gas burners, following a thermal cycle (Figure 3) with a total time of 50 minutes and 5-minute dwell at a peak temperature of 1190ºC. The fired bodies, once at ambient temperature, were characterised again with the non-destructive inspection equipment using X-ray absorption, determining their bulk density and thickness distributions. In addition, using dimensional characterisation equipment, their dimensional characteristics were determined in accordance with standard UNE-EN ISO 10545-2:1998.

3 RESULTS AND DISCUSSION

The results obtained during the determination of the viscous law for the porcelain tile composition used and the reproduction of its behaviour on an industrial scale are described below.

3.1 OBTAINMENT OF APPARENT VISCOSITY, H_0

Figure 2 (right) and equations (1) and (2) enable apparent viscosity (η_0) to be isolated in order solely to plot its dependence on temperature. To do so, the parameters corresponding to grain growth were fitted, using a multiparameter optimiser developed in Python™, to assure that η_0 was independent of the material's microstructure during sintering.

The variation with temperature of the experimental apparent viscosity of the porcelain tile composition used, for the three test values of ρ_0, is shown in Figure 6. The three curves exhibited similar behaviour, with an exponential decrease in the logarithm of viscosity with temperature from 850ºC on, and a less pronounced decrease in viscosity from 1000ºC on. The results indicate that the variation in tile viscosity with temperature did not properly fit an Arrhenius law, given the complexity involved of the physical and chemical transformations.

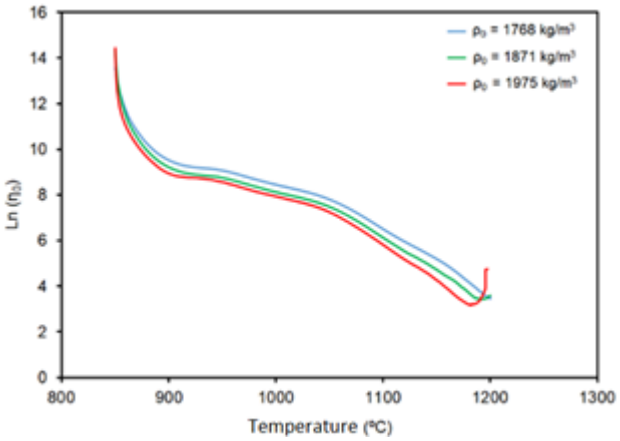

***Figure 6**. Experimental apparent viscosity of the porcelain tile composition as a function of its initial bulk density.*

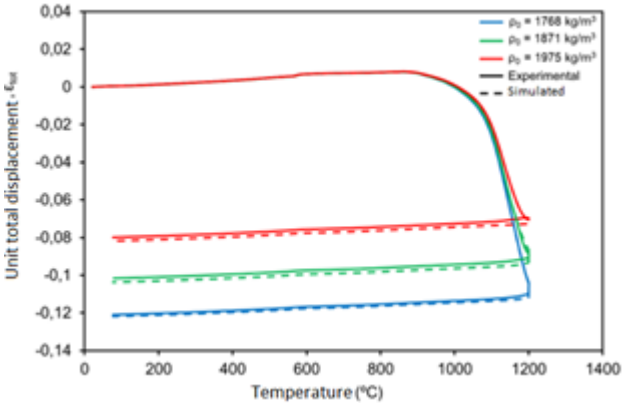

***Figure 7**. Comparison of the experimental and simulated dilatometric plots with the proposed viscous law.*

Moreover, around peak firing temperature, a sharp increase in viscosity was observed, which rose as the value of ρ_0 increased, which was due to a numerical artifice associated with the overshoot observed in Figure 2 (right). This problem could be minimised by extrapolating the straight section of Figure 6 located between 1100 and 1150ºC.

With this viscous law, the dilatometric plots of Figure 2 (left) could be accurately reproduced, as shown in Figure 7. Note how the main differences between the experimental and simulated results emerged at cooling start, resulting from the extrapolation made to minimise the effect of the overshoot described above.

3.2 INDUSTRIAL VERIFICATION OF THE METHODOLOGY

Figure 8 shows the thickness maps of the fired bodies, obtained by non-destructive analysis of these bodies, compared with those resulting from simulation of their behaviour by solution of the SOVS model, for the industrial thermal cycle used. Good agreement may be observed between the experimental data and the simulations, in both cases, test pieces 1X and 2X exhibiting the greatest heterogeneities, as was to be expected.

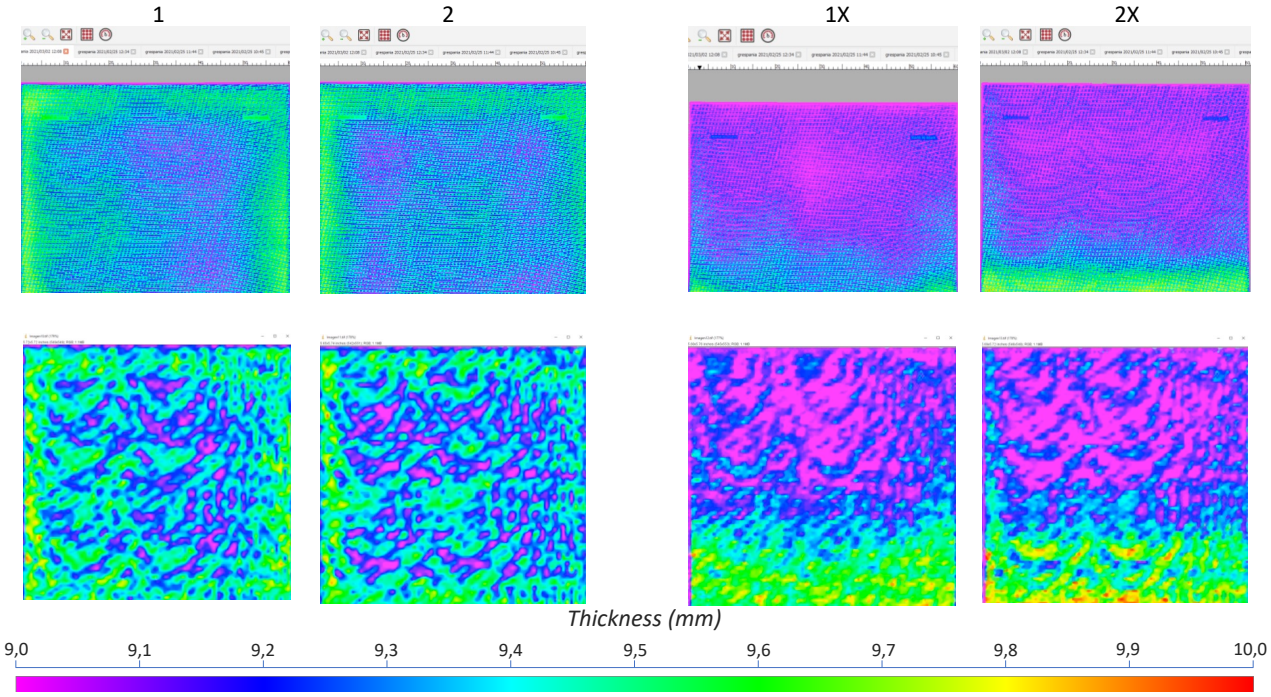

Figure 8. *Experimental maps (top part) of the thickness distribution of the fired bodies compared with those resulting from the simulations (bottom part).*

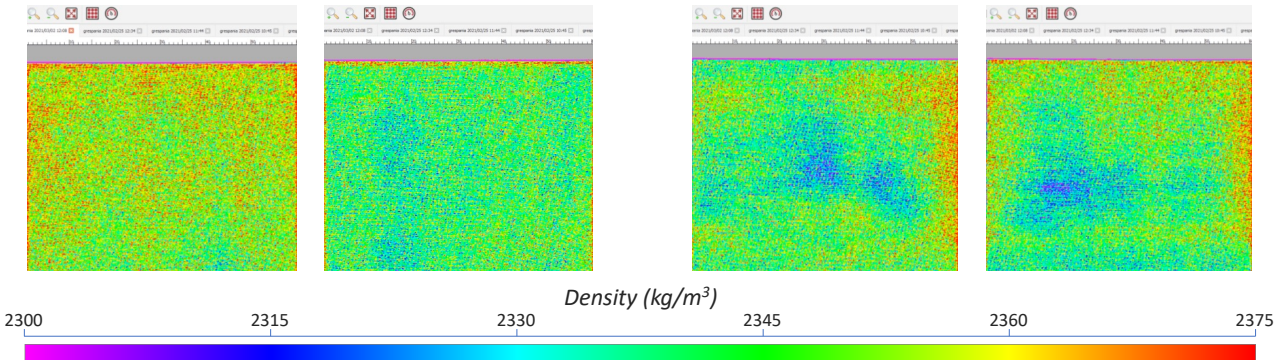

Figure 9. *Experimental maps of bulk density distribution of the fired bodies.*

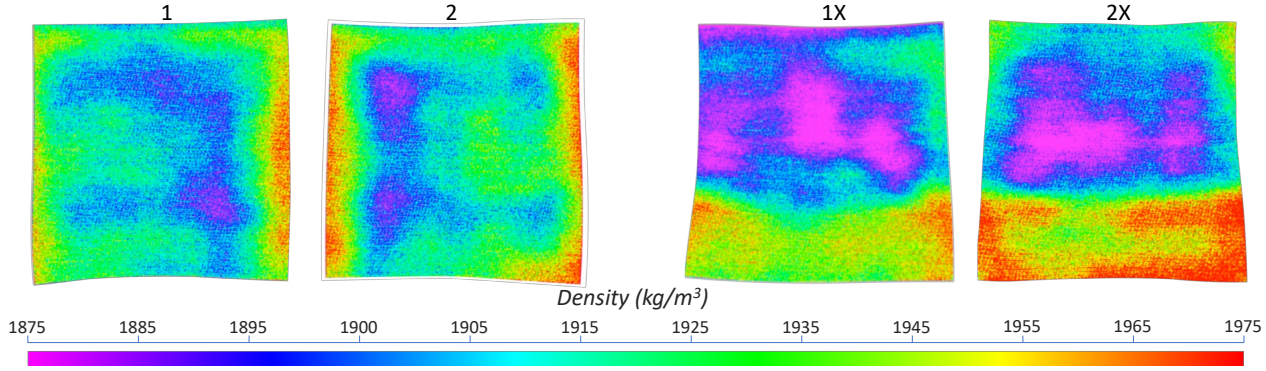

Figure 10. *Simulated final morphology of the fired bodies obtained by magnifying 5x the displacements during the sintering process.*

The bulk density distribution maps of the fired bodies obtained by X-ray absorption are depicted in Figure 9. Compared with the dry bulk density maps, they were noticeably more uniform, as sintering tended to make the porosity distribution in the material more uniform, at the expense of generating differences in shrinkage, which were more pronounced as the initial heterogeneities in density increased. This same occurred in the images shown in Figure 10, in which the final simulated morphology of the four bodies is depicted. For illustrative purposes, the strains have been magnified 5x, and the map of the bulk density of the dry body has been included on the morphology. It may be observed that, in every case, the predicted strains matched the experimentally determined bulk density distribution.

To assess the accuracy of the model in the estimation of the final dimensions of the test pieces, the results provided by the model were compared with the experimental measurements on the fired bodies. Specifically, the mean thicknesses of 5-cm wide borders parallel to each of the sides of the test pieces were compared, as was the length of each of the sides in accordance with standard UNE-EN ISO 10545-2:1998. The experimental dimensions have been plotted versus those predicted by the simulation model in Figure 11. The fit between the experimental data and the simulated data was good, with an absolute error in the thickness estimation for a level of confidence of 95% of ±0.09 mm and of ±2 mm in the estimation of side length. The accuracy in the length estimation was relatively low. However, observing the pieces as a whole, the predictions provide information of great value for understanding how the tiles will behave during firing.

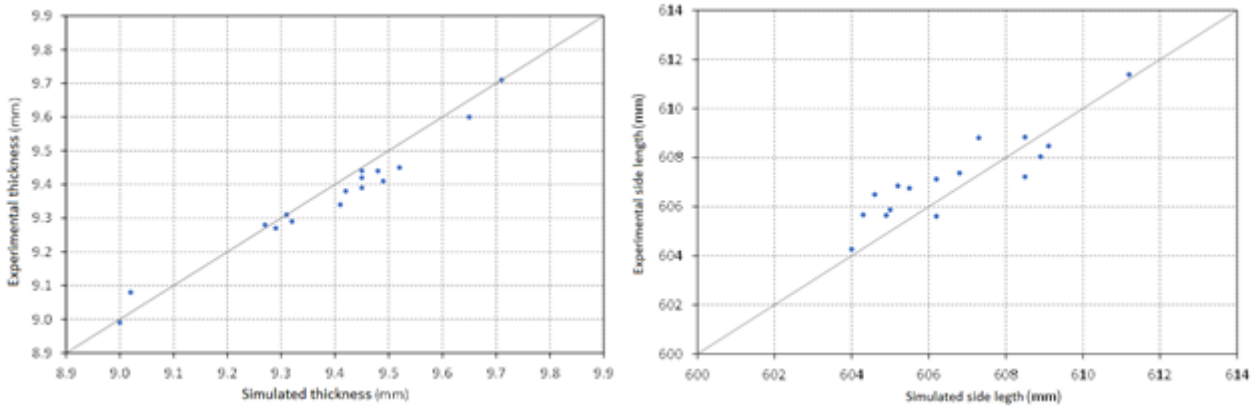

Figure 11.*Comparison between the experimental dimensions of the pieces (left: thicknesses; right: side length) and the ones predicted by the simulation model.*

Finally, Table 1 details the calculation times used for each industrial simulation performed. The computer equipment used had a 32 core processor Intel© Core™ i9-7960X at 2.8GHz and 128Gb Memory RAM DDR4-2666, for each simulation using 4 processing cores and 3.5 Gb RAM. It is to expected that, with current technologies, these simulation times could be readily reduced to 2 h.

Simulation	Calculation time (h)
1	5.02
1X	5.04
2	5.04
2X	5.05

Table 1. Calculation time for each simulation of the industrial bodies.

4. CONCLUSIONS

The following conclusions were drawn from the present study:

- It is possible to reproduce the behaviour of a porcelain tile body during sintering using the modified SOVS model and an experimental viscous law.

- It is feasible to use the SOVS model to simulate the firing behaviour of industrial porcelain tiles from their thermo-mechanical properties and from their thickness and dry bulk density distribution maps.

- The calculation times provided by current calculation systems would allow the proposed simulation methodology to be used for routine prediction of porcelain tile behaviour during the firing process, anticipating the appearance of defects, fundamentally of a dimensional character.

4. REFERENCES

[1] SÁNCHEZ, E.J. Consideraciones técnicas sobre el producto y el proceso de fabricación del gres porcelánico. Cerámica Información, 285, 73–91, 2002.
[2] AMORÓS, J.L.; CASTRO-LOPES, F.; CERISUELO, J.A.; LLORENS, D.T.; MALLOL, J.G.; MEZQUITA, A.; VARGAS, M. Mejora de la estabilidad dimensional de piezas de gres porcelánico a través de la medida en continuo de la humedad de los soportes prensados. Cerámica Información, 311, 117–126, 2004.
[3] BOIX, J.; DACHAMIR HOTZA; DOLLY SANTOS; MALLOL, J.G. Dimensional changes of porcelain tiles under different processing conditions. Part I: Laboratory-Scale models. Ceramics International
[4] BALAGUER, J.; TISCAR, J.M.; SABURIT, A.; QUEREDA, F.; AGUILELLA, M. Modelización de la sinterización de baldosas cerámicas mediante el modelo SOVS. QUALICER PROCEEDINGS 2020, 2020.
[5] ARGÜELLO, J. et al.; Verification, Performance, Validation, and Modifications to the SOVS Continuum Constitutive Model in a Nonlinear Large-Deformation Finite Element Code. July 2009, Journal of the American Ceramic Society; 92(7):1442–1449
[6] AMORÓS, J.L.; BOIX, J.; FELÍU, C.; FUENTES, I.H.; LLORENS, D.T.; MALLOL, J.G. Non-destructive measurement of bulk density distribution in large-sized ceramic tiles. J. Eur. Ceram. Soc., 30, 2927–2936, 2010.
[7] SKOROHOD, V.V., Rheological basis of the theory of sintering, Naukova Dumka, Kiev, 1972
[8] CANTAVELLA, V. (1998). Simulación de la deformación de baldosas cerámicas durante la cocción. Universitat Jaume I.

ACKNOWLEDGEMENTS

The authors of this study thank the Valencian Institute for Business Competitiveness (IVACE) for the economic support provided, through the European Regional Development Fund (ERDF), for enabling this research to be carried out via the aid programme for Technology Centres of the Valencia Region for the conducting R&D projects.